sustainability

MDPI

Article

A Comparative Study in Vanadium and Tungsten Leaching from Various Sources of SCR Catalysts with Local Difference

Qingfa Su [1,2,3], Xianfang Yi [1,2,3], Jifa Miao [1,2,3], Yanting Chen [1,2], Jinsheng Chen [1,2,*] and Jinxiu Wang [1,2,*]

1 Center for Excellence in Regional Atmospheric Environment, Institute of Urban Environment, Chinese Academy of Sciences, Xiamen 361021, China; qfsu@iue.ac.cn (Q.S.); xfyi@iue.ac.cn (X.Y.); jfmiao@iue.ac.cn (J.M.); ytchen@iue.ac.cn (Y.C.)

2 Key Laboratory of Urban Environment and Health, Institute of Urban Environment, Chinese Academy of Sciences, Xiamen 361021, China

3 University of Chinese Academy of Sciences, Beijing 100049, China

* Correspondence: jschen@iue.ac.cn (J.C.); jxwang@iue.ac.cn (J.W.)

Received: 18 January 2020; Accepted: 14 February 2020; Published: 18 February 2020

Abstract: Direct leaching with NaOH can be an economically acceptable method for vanadium (V) and tungsten (W) recovery from spent selective catalytic reduction (SCR) catalysts. However, different chemical-physical characteristics of catalysts would affect the V and W leaching. In this paper, the V and W leaching behavior of various sources of SCR catalysts with a local difference (yellow and gray color) were systematically investigated with alkali leaching solution under ambient pressure. Different leaching efficiencies from yellow and gray color areas were correlated with oxidation states and species of V and W on catalyst surfaces, as characterized by X-ray photoelectron spectroscopy (XPS), Raman, Fourier transform infrared spectroscopy (FTIR), and other analytic methods. For the V leaching efficiency, the samples from a gray area of catalysts (40.0–51.0%) were lower than that from the yellow area (66.8–69.8%). The higher molar ratio of V^{3+} and a lower molar ratio of V^{5+}, and the lower total V content on the surface of the samples from the gray area could be the main reasons for the lower V leaching efficiency. As for the W leaching efficiency, the samples from the gray area (44.6–57.3%) were slightly higher than that from the yellow area (38.0–52.6%) of catalysts. The less total W content of surface species and stronger interaction among V–W–Ti of yellow area samples resulted in the lower leaching efficiency. These differential leaching efficiencies needed to be taken into consideration for recovering V and W from spent SCR catalysts.

Keywords: vanadium leaching; tungsten leaching; local difference; color difference; catalyst characterization

1. Introduction

The selective catalytic reduction (SCR) technology is the most efficient and industrially widespread technology for reducing NO_x emission from stationary sources [1,2]. For decades, as a mature catalyst with a high NO_x conversion rate, a wide operating temperature window, and excellent stability, a considerable amount of V_2O_5-WO_3/TiO_2 catalysts have been installed in the SCR system. Final disposal, such as landfill or recovery for other uses, is unavoidable after catalyst operating life [3,4].

As a hazardous solid waste, the landfill disposal cost is relatively high. Thus, various approaches have been developed for recovering valuable metals from spent SCR catalysts. As compared with high-temperature roasting or high-pressure leaching method, which means high energy cost and leads to a high concentration of impurities in leaching solutions, such as silicon, Na_2TiO_3, $Na_2Ti_3O_7$ [5–7],

direct leaching with alkali solution under ambient pressure seems more economically acceptable. There are only a few research studies on direct leaching by alkali under ambient pressure (Table 1); all the researches are carried out with specific catalyst, and the leaching efficiency is quite different among the various researches. Furthermore, most of the researches focused on the influence of leaching parameters, such as temperature, time, concentration, liquid/solid ratio, particle size, and stirring speed. Wu et al. [8] reported that the leaching efficiency of vanadium (V) and tungsten (W) was optimized at 87% and 91%. Tang et al. [9] declared that the leaching efficiency could be as high as 93% for V and 97% for W. Su et al. [10] reported that the leaching efficiency was only 66% for V and 49% for W. All these researches were carried out with a specific catalyst, and the leaching rates were quite different among the various researches. Different leaching rates are not only because of different methods but also different catalysts. Because the commercial SCR catalyst is produced by different manufacturers, using various formulation and processes, and then they are serviced under different operating conditions. Therefore, different catalysts may have different chemical-physical characteristics [11,12], which would affect V and W leaching efficiency. Also, V atoms easily lose electrons and form three different valences state (V^{5+}, V^{4+}, and V^{3+}) in the SCR catalyst, and vanadium oxides exist in the forms of monomeric, polymeric, or crystalline [13–15]. Besides, although the commercial catalysts are usually in light yellow and uniform, some extracted catalysts are non-uniform in color, and even there is a gray cylindrical region through the axle center of each catalyst [11]. It is concerned that whether this variation would influence V and W leaching to some degree. However, a comparative study and the reasons why different catalysts have different leaching behaviors have not been reported in the literature.

Table 1. The vanadium (V) and tungsten (W) leaching efficiency of selective catalytic reduction (SCR) catalyst by direct leaching method reported in the literature.

Ref.	Reagents	Temperature (°C)	Time (min)	Particle size (μm)	Efficiency (%)
Wu et al. [8]	NaOH	70	30	74	V: 87, W: 91
Tang et al. [9]	NaOH	100	180	150	V: 93, W: 97
Su et al. [10]	NaOH	100	90	150	V: 66, W: 49
Li et al. [4]	NH_4HCO_3+H_2O_2	80	180	45	V: 95; W: 98
Li et al. [16]	H_2SO_4	80	120	74	V: 42
Zhang et al. [17]	H_2SO_4+Na_2SO_3	95	120	74	V: 100
Wu et al. [18]	oxalic acid	90	180	75	V: 84

This work focused on the different leaching behaviors of V and W between the yellow and gray color areas in various sources of SCR catalysts with local differences. The leaching efficiency of V and W from the yellow and the gray area samples were tested under the same condition based on the previous work [10]. Also, the reasons why the yellow and the gray area samples from the same one catalyst show different leaching behaviors were discussed based on the characterizations.

2. Materials and Methods

2.1. Sample Preparation

The commercial honeycomb catalyst was obtained from coal-fired power plants. All the selected catalysts had a gray cylindrical region through the axle center (Figure 1a). S1 and S2 were fresh catalysts; S3, S4, and S5 were spent catalysts. The solids deposited on the SCR catalysts were physically removed by compressed air (0.5 MPa), the yellow area and the gray area were carefully separated manually, and the color transition part was discarded. Then, the samples from the yellow area and the gray area were pulverized by a hammer, ground by the vibration mill (LDP-750A; Hongtaiyang, Yongkang, China), and sieved after drying them to the constant weight. Finally, the SCR catalyst samples with particle size smaller than 100 meshes were obtained. The tested samples extracted from a gray area were labeled as "G", which means gray (Figure 1b), and that from a yellow area labeled as

"N", which means normal (Figure 1c). For example, S1G means the sample from the gray area of the S1 catalyst, and S2N means that from the yellow area of the S2 catalyst.

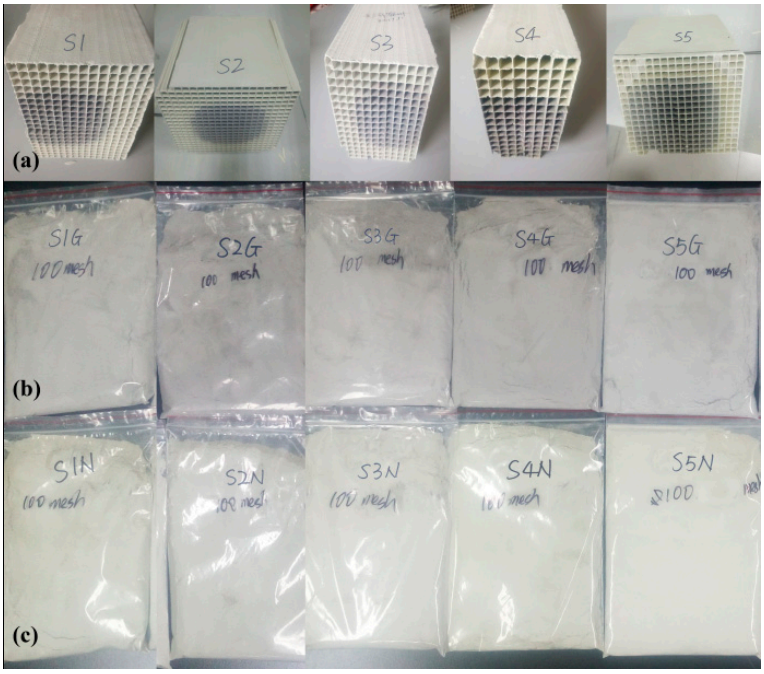

Figure 1. Photos of catalysts (**a**); the tested particle samples extracted from the gray area (**b**) and yellow area (**c**) of the catalysts with color variation, respectively.

2.2. Leaching

A chosen condition based on the previous work [10] (temperature 100 °C, liquid/solid (L/S) 15, stirring speed 900 rpm, NaOH concentration 1.5 mol/L, leaching time 120 min) was utilized to evaluate the different leaching behaviors among all the various samples. The leaching tests were performed in a 50 mL Teflon tube immersed in an oil bath with magnetic stirring at a required temperature (±0.5 °C). After leaching, the slurry was sampled and separated by vacuum filtration, and then the clear liquid was filtered with a 0.22 μm membrane filter. The cake was washed sufficiently with deionized water by vacuum pump until the pH of the filtrate was lower than 8. Then, the cake was dried at 105 °C for 24 h.

2.3. Analysis

The concentration of V and W in the leaching solution was measured by an inductively coupled plasma optical emission spectrometer (ICP-OES, Optima 7000DV, Waltham, MA, USA). The elemental analysis of catalysts and residuals was conducted on an X-ray fluorescence spectrometer (XRF, Axios mAX, PANalytical B.V., Almelo, Holland). As considering the deviation of XRF, the V and W content of original catalysts were corrected by a wet method. A 0.1 g catalyst was added to 6 mL digestive solution composed of hydrochloric acid, nitric acid, and hydrofluoric acid with ratio 3:2:1 in a closed digestion vessel and digested in a graphite digestion instrument. Then, the solution was analyzed by ICP-OES, and the results were used to calculate the leaching efficiency by using Equation (1):

$$\text{Leaching efficiency, } \% = \frac{VC_i}{mw_i} \times 100 \quad (1)$$

where C_i is the concentration of V and W in the leaching solution; V is the volume of the leaching solution; m is the mass of the initially added spent SCR catalyst; W_i is the content of V, and W is the initially added spent SCR catalyst.

2.4. Characterization

The crystalline phase of samples was detected by X-ray diffraction (XRD, X'Pert Pro, PANalytical B.V., Almelo, Holland) at 40 kV and 40 mA with Cu Kα ray. The elemental valence was detected by X-ray photoelectron spectroscopy (XPS) analysis, which was collected on an ESCALAB 250Xi photoelectron spectrometer (Thermo Fisher Scientific, Waltham, MA, USA) with monochromatic Al Kα radiation (E = 1486.2 eV) using the binding energy (284.8 eV) of amorphous carbon C 1s as a reference point. The further analysis of the XPS spectra of samples was conducted by "Avantage" software supplied by Thermo Fisher Scientific Corporation, and uses the "Scofield factor" as a sensitive factor. The specific surface areas and pore size distributions were determined by N_2 adsorption/desorption isotherms at 77K with Brunanuer–Emmett–Teller (BET) and Barrett–Joyner–Halenda (BJH) methods (Quantachrome Corp., Boynton Beach, FL, USA). Raman analysis was conducted by a Laser Raman spectrometer (LabRAM Aramis, Horiba Jobin Yvon, Paris, France). The Fourier transform infrared spectra (FTIR) of the catalysts were recorded on Bruker Vertex 70 infrared spectrometer (Bruker, Karlsruhe, Germany).

3. Results

3.1. Vanadium and Tungsten Leaching Behavior

Figure 2 shows the V leaching efficiency of yellow and gray areas from five different kinds of catalysts. The sequence of leaching efficiency of V from yellow samples was S1N (69.8%) ≈ S2N (69.7%) > S4N (68.8%) > S5N (67.7%) > S3N (66.8%), and this was similar to the result of our previous work in which the V leaching efficiency from catalyst without color difference was about 66.3%. As for gray samples, the leaching efficiency was much lower and in the following sequence: S1G (51.0%) > S2G (49.1%) ≈ S5G (49.0%) > S3G (42.1%) > S4G (40.0%). Thus, it could be concluded that the V leaching efficiency from the yellow area was higher (67–70%) than that from the gray area (40–51%).

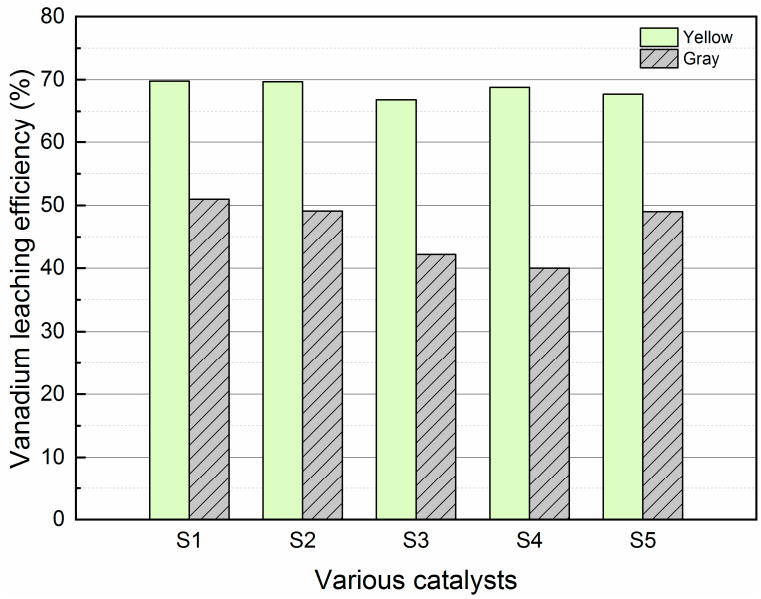

Figure 2. Vanadium leaching efficiency of the yellow and the gray area samples from fresh (S1 and S2) and spent (S3, S4, and S5) catalysts.

The W leaching efficiency of yellow and gray areas from five different kinds of catalysts are shown in Figure 3. For yellow area samples, the sequence of leaching efficiency of W was: S4N (52.6%) > S5N (44.7%) > S1N (44.2%) > S2N (41.4%) > S3N (38.0%), and this was similar to the result of our previous work in which the W leaching efficiency from catalyst without color difference was about 48.5%.

The gray area samples had similar sequence: S4G (57.3%) > S1G (54.2%) > S5G (53.2%) > S2G (52.0%) > S3G (44.6%). S3N showed the lowest leaching efficiency of about 38.0%, and S4G had the highest leaching efficiency (57.3%). Opposite to the leaching behaviors of V, the W leaching efficiency of the yellow area samples (38.0–52.6%) was slightly lower than that of the gray area samples (44.6–57.3%).

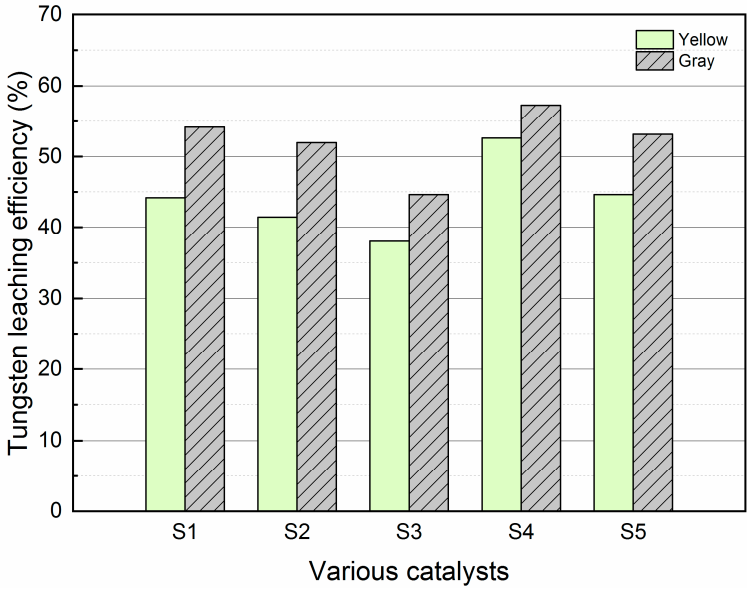

Figure 3. Tungsten leaching efficiency of the yellow and the gray area samples from fresh (S1 and S2) and spent (S3, S4, and S5) catalysts.

3.2. Chemical and Textural Characterizations

XRD was used to analyze the composition and phase structure of the ten samples. As shown in Figure 4, all the diffraction peaks could be indexed to anatase TiO_2 only, and neither V_2O_5 nor WO_3 was detected among all the samples. The absence of these bulk phases in the XRD patterns implied that V and W species were present in either non-crystalline state or lower content than the detection limit of XRD.

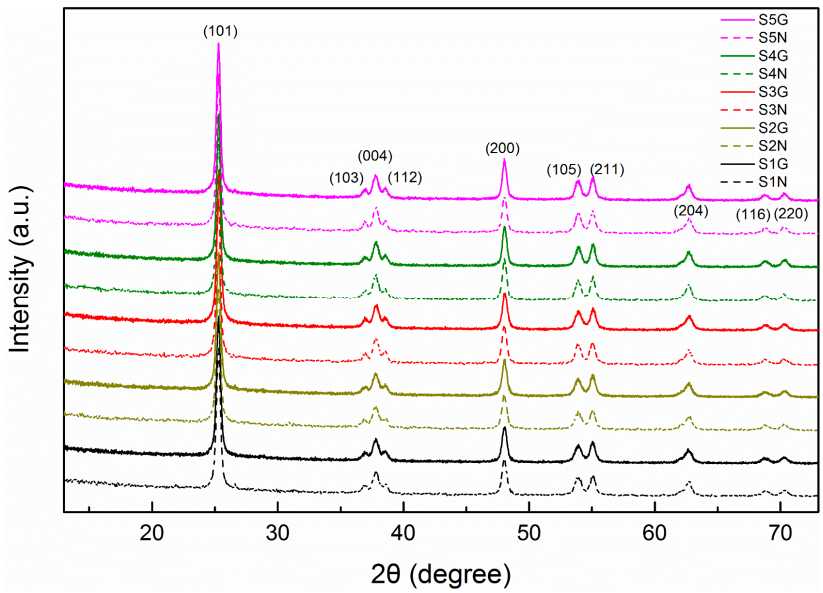

Figure 4. X-ray diffraction (XRD) patterns of samples.

As seen in Table 2, the elemental composition of all the samples included TiO_2, V_2O_5, WO_3, SiO_2, CaO, and Al_2O_3, which was totally higher than 95%. These main components of two samples from yellow and gray areas from one catalyst were similar. Moreover, there were apparent differences in V and W contents among various sources catalysts as a result of manufacture formulations or the V and W loss to varying extents after the serving time.

Table 2. The chemical compositions of catalysts (wt.%).

Catalysts	V_2O_5 [a]	WO_3 [a]	TiO_2 [b]	SO_3 [b]	SiO_2 [b]	CaO [b]	Al_2O_3 [b]
S1G	1.036	4.761	76.970	0.425	9.354	2.768	2.288
S1N	1.015	4.685	76.817	2.261	8.168	2.542	1.984
S2G	1.005	4.798	77.939	0.433	8.835	2.772	2.252
S2N	0.985	4.632	76.777	2.300	7.905	2.475	1.875
S3G	0.925	4.453	81.726	1.113	7.162	1.828	1.005
S3N	0.909	4.392	81.590	1.386	7.285	1.775	1.072
S4G	0.554	2.222	88.410	1.544	3.816	1.165	0.984
S4N	0.550	2.234	88.687	1.559	3.777	1.180	0.979
S5G	0.749	3.154	78.149	1.875	9.293	2.988	2.435
S5N	0.735	3.146	78.185	2.785	8.367	2.903	2.153

[a] results of inductively coupled plasma optical emission spectrometer (ICP-OES), [b] results of X-ray fluorescence spectrometer (XRF).

Table 3 lists the textural properties of catalysts, including surface area, pore-volume, and pore diameter. There were slight differences between gray and yellow area samples among all the catalysts, and the range of specific surface area from 40.3 m^2/g to 56.7 m^2/g was mainly caused by different formulations for sampled catalysts. Dong et al. prepared SCR catalysts under different oxygen content atmospheres, and the color of samples changed from yellow to gray when the oxygen content decreased [19]. Also, the lower specific surface area of the yellow sample than the gray sample might be due to the sufficient oxidation of V and W.

Table 3. The textural properties of catalysts.

Catalysts	Specific Surface Area (m^2g^{-1})	Pore Volume (cm^3g^{-1})	Average Pore Radius (nm)
S1G	48.90	0.26	10.6
S1N	46.22	0.24	10.4
S2G	48.02	0.22	9.3
S2N	44.02	0.22	10.1
S3G	49.61	0.24	9.7
S3N	41.26	0.24	11.4
S4G	56.65	0.27	9.4
S4N	54.95	0.26	9.5
S5G	40.40	0.22	10.1
S5N	40.34	0.21	10.4

3.3. XPS Analysis

As shown in Figure 5a, the binding energy of Ti $2P_{3/2}$ (458.7 eV) was attributed to the typical characteristic peak of Ti^{4+} ion. Chen et al. and Zhang et al. concluded that the Ti^{4+} would shift to higher binding energy after adding WO_3 [20,21]. The lower binding energy of Ti^{4+} (458.4 eV) was found on both S1G and S2G, indicating weak interaction between WO_3 and TiO_2. A similar phenomenon was found on O1s (Figure 5b) and W_{4f} (Figure 5c), for S1G and S2G; the O1s binding energy shifted from 530 to 529.6 eV, and the W_{4f} shifted to lower binding energylevels by 0.3 eV.

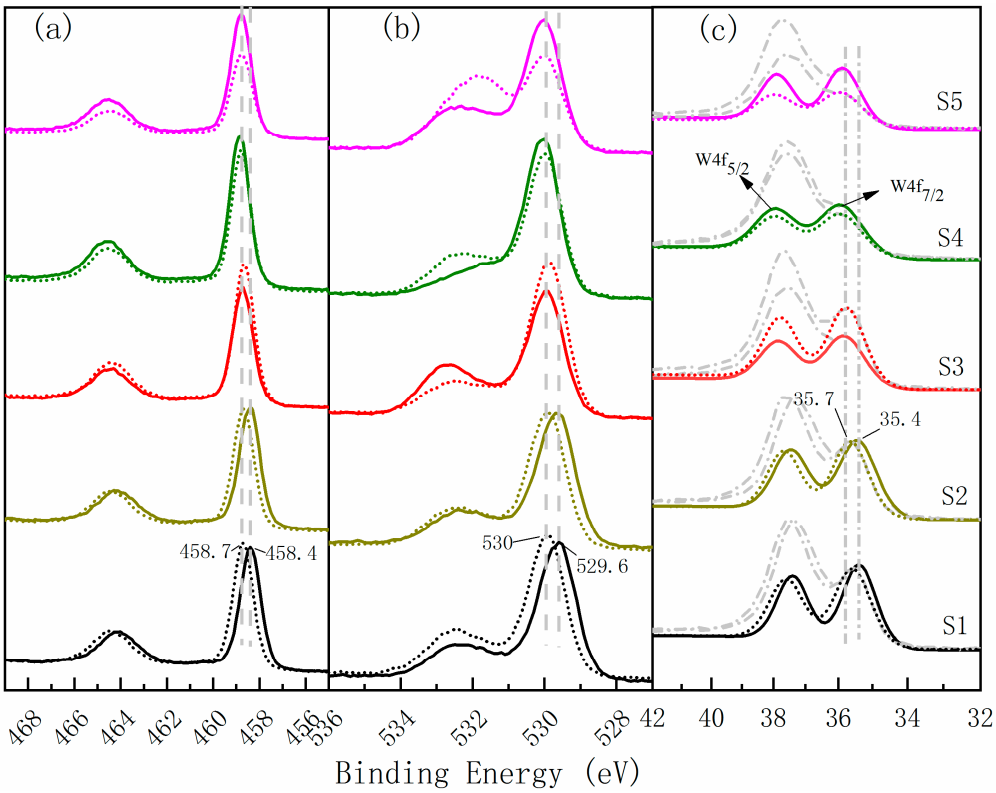

Figure 5. X-ray photoelectron spectroscopy (XPS) spectra of catalysts before leaching (solid—gray samples, dotted—yellow samples): Ti 2p (**a**), O 1s (**b**), and W 4f (**c**) (the gray line—the envelope of W 4f Peaks and Ti 3p peaks).

It is well known that the existing form of V in the commercial SCR catalyst is rather intricate. It could exist as dispersed monolayer isolated vanadyl [12], polymeric surface VO_x species [20,22], V species in oligomeric structure [23]. Also, V can enter into the TiO_2 crystal lattice due to the very close ionic radius of V^{4+} to that of Ti^{4+} [24].

XPS was used specifically to analyze the surface compositions and oxidation states of all the catalysts. The V $2p_{3/2}$ spectra were resolved into three peaks [25] (Figure 6), and the molar ratios of V^{5+}, V^{4+}, and V^{3+} are shown in Table 4. The bulk (measured by XRF and ICP) and the surface (performed by XPS) molar compositions of all the samples are listed in Table 4. As shown in Table 4, the bulk amounts of V and W were similar between gray and yellow area samples, and lower than surface amounts. It implied that the V and W species migrated from internal onto the surface during the calcine or reaction phase [11,20].

For V species, the surface amounts of gray samples were lower than that of yellow samples for all catalysts. Nevertheless, for W species, that was the opposite. According to the well-known shrinking core models [9,26], the higher surface amounts of V on the yellow samples and W on the gray samples could be one of the reasons that the yellow samples showed higher V leaching efficiency but lower W leaching efficiency.

For all catalysts, the ratios of the V^{3+} valence state of the gray area samples were higher than that of yellow area samples, and the ratios of the V^{5+} valence state of the gray area samples were lower than that of yellow samples. It is known that the colors of vanadium oxides vary with the change in the valence of V. Yaws et al. [27] mentioned that V_2O_3 is black color, VO_2 is blue-black color, and V_2O_5 shows yellow-brown color. As shown in Figure 1, all the selected catalysts had locally different colors, and the samples from gray areas contained higher V^{3+} or V^{4+} species (V_2O_3 and VO_2) than that from yellow areas; this might be caused by inadequate oxygen supply, resulting in insufficient oxidation of V in the gray area during the sintering process [11,19]. As compared with amphiprotic oxide VO_2

and V_2O_5, V_2O_3 is hardly solved in alkaline or acid, and then additional oxidation is usually used to enhance vanadium leaching [18,28–31]. Thus, the higher molar ratios of V^{3+} and lower molar ratios of V^{5+} valence could be another reason for the lower V leaching efficiency of gray samples.

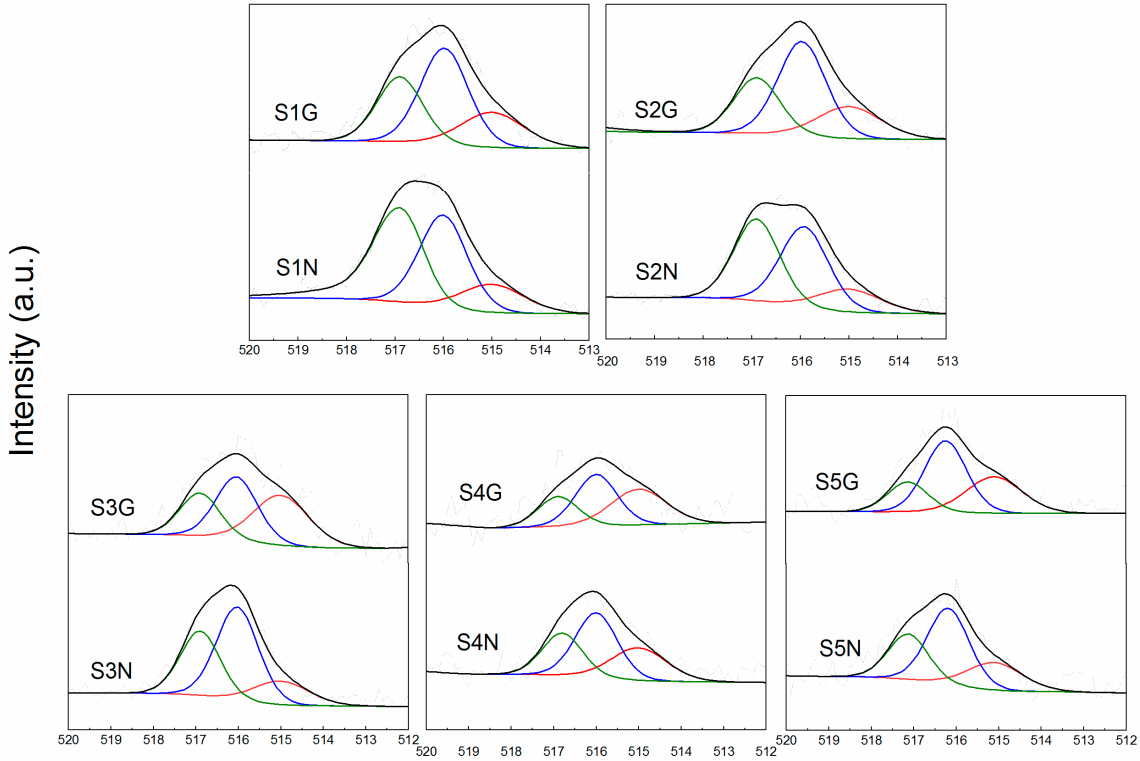

Figure 6. XPS spectra results (before leaching) of V 2p3/2 by the curve fitting method.

Table 4. Surface and bulk analysis of catalysts and the results of V $2P_{3/2}$ peak fitting.

Samples	Surface Atom Ratio (% mol/mol)			V $2P_{3/2}$ Peak Fitting			Bulk Analysis (% mol/mol)		
	Ti	V	W	V^{3+}	V^{4+}	V^{5+}	Ti	V	W
S1G	87.76	3.00	9.24	22.63	46.96	30.41	96.91	1.10	1.99
S1N	87.10	3.96	8.94	15.42	38.59	45.99	96.96	1.08	1.96
S2G	88.34	2.65	9.01	22.22	49.64	28.14	96.96	1.06	1.98
S2N	87.87	3.70	8.42	15.96	42.60	41.46	97.01	1.05	1.94
S3G	90.63	1.74	7.63	38.76	36.98	24.26	97.31	0.93	1.76
S3N	89.61	3.08	7.31	16.78	50.02	33.20	97.35	0.92	1.74
S4G	93.07	1.03	5.89	37.25	40.20	22.55	98.66	0.52	0.82
S4N	93.49	1.42	5.09	29.04	43.65	27.31	98.66	0.52	0.82
S5G	91.39	1.63	6.98	32.51	48.19	19.30	97.90	0.79	1.31
S5N	91.90	2.48	5.62	23.27	48.78	27.95	97.92	0.78	1.31

Also, the XPS spectra results of Ti 2p (Figure 7a) and O 1s (Figure 7b) before and after leaching are displayed. Except for S1G and S2G with lower Ti2p and O1s binding energy before leaching, other catalysts obviously shifted to lower binding energy after leaching. Ti 2p binding energy shifted from 458.7 to 458.4 eV, and O 1s binding energy shifted from 530.0 to 529.6 eV, indicating that the surface W species was leached. This was consistent with the phenomenon found by Chen et al. and Zhang et al. that the modification with WO_3 results in the Ti^{4+} shift to higher binding energy [20,21].

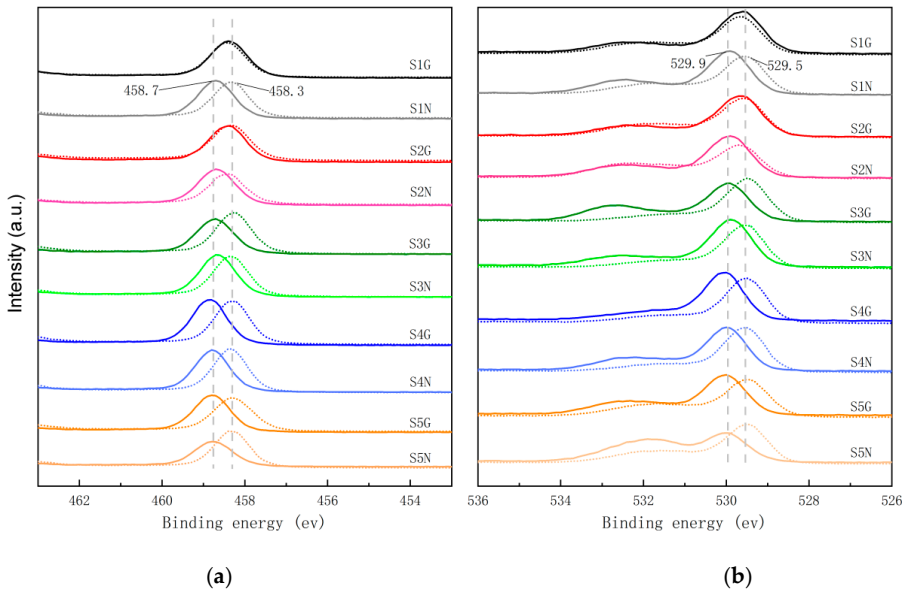

(**a**) (**b**)

Figure 7. XPS spectra of catalysts before (solid) and after (dotted) leaching: Ti 2p (**a**), O 1s (**b**).

3.4. Raman Analysis

As shown in Figure 8a, the vibrations at 196 cm^{-1}, 397 cm^{-1}, 518 cm^{-1}, and 636 cm^{-1} were fingerprint peaks of anatase TiO_2. To get more details, the Raman active modes in the range of 750~1200 cm^{-1} were also investigated and shown in Figure 8b. All the catalysts showed a peak at 798 cm^{-1}, which could be assigned to the Ti-O vibration of TiO_2 or crystal tungsten oxide [19,20]. The broadband between 925 cm^{-1} and 1000 cm^{-1} could be indexed to the overlap of contributions from polymeric vanadate species and both tetrahedrally and octahedrally coordinated polymeric WO_x [14,19,32]. In the FTIR spectra (Figure 9), all the samples had a significant vibration band at 1050 cm^{-1}, which was related to W=O stretches [17]. It also could be found that there was a peak at 1016 cm^{-1} in the samples with high sulfur content according to XRF and XPS, which might be assigned to the vibration of sulfate [14], and this was consistent with FTIR results showing that there was a vibration band at 1121 cm^{-1} (Figure 9) [17]. As compared with gray samples, the peak between 925 and 1000 cm^{-1} of yellow samples was broader and higher, meaning that there is much stronger interaction among W, V, and Ti species [20]. The stronger interaction between W species and TiO_2 anatase lattice could result in lower W leaching efficiency [5]. Thus, the stronger interaction among V–W–Ti and the less content of surface W species of yellow area samples might result in their lower W leaching efficiency.

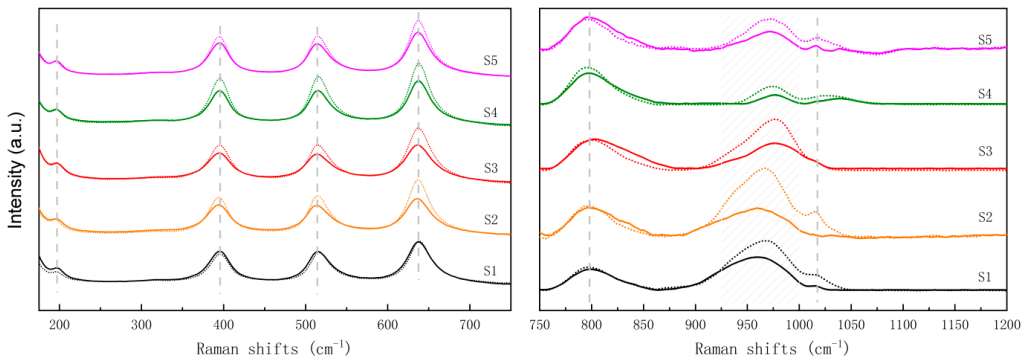

(**a**) (**b**)

Figure 8. Raman spectra of catalysts (solid—gray samples, dotted—yellow samples) in a range of (**a**) 175–750 cm^{-1} and (**b**) 750–1200 cm^{-1}.

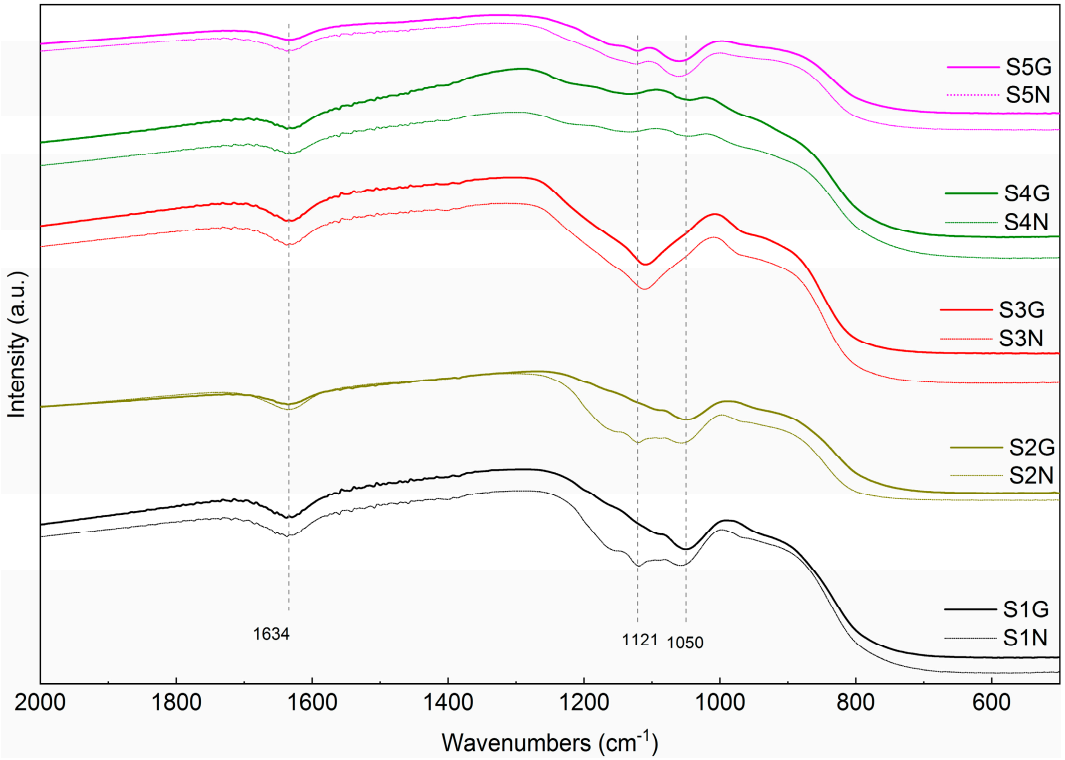

Figure 9. Fourier transform infrared spectroscopy (FTIR) spectra of catalysts.

4. Conclusions

The leaching behaviors of V and W for five catalysts with the local color difference were systematically investigated under a specific condition (100 °C, NaOH concentration 1.5 mol/L, L/S 15, stirring speed 900 rpm, time 240 min, and atmosphere pressure). For V, the leaching efficiency of samples from the gray part (40.0–51.0%) was lower than that from the yellow part (66.8–69.8%). On the contrary, the W leaching efficiency of samples from the gray part (44.6–57.3%) was higher than that from the yellow part (38.0–52.6%). According to surface characterization, the higher molar ratio of V^{3+} and a lower molar ratio of V^{5+} valence, and the lower total V content on the surface of samples could be the main reasons for that gray area samples to had lower V leaching efficiency than yellow area samples. For W leaching, as compared with the gray area samples, the stronger interaction among V–W–Ti and the less W content of surface species of yellow area samples might result in lower leaching efficiency. Therefore, the spent catalysts with local color differences require special attention when they are leached to recycle V and W. The color sorting technology or developing efficient leaching method might be considered based on the economy.

Author Contributions: Conceptualization, Q.S. and J.C.; Data curation, J.W.; Investigation, Q.S., X.Y., and J.M.; Resources, Y.C.; Supervision, J.C. and J.W.; Writing—original draft, Q.S.; Writing—review and editing, J.C. and J.W. All authors have read and agreed to the published version of the manuscript.

Funding: This research is funded by Youth Innovation Promotion Association, Chinese Academy of Sciences (grant number 2020309), and the Strategic Priority Research Program of the Chinese Academy of Sciences (XDB05050500).

Acknowledgments: We thank Muh-cheng Milton Wu for his linguistic assistance during the preparation of this manuscript.

Conflicts of Interest: The authors declare no conflict of interest.

References

1. Marberger, A.; Ferri, D.; Rentsch, D.; Krumeich, F.; Elsener, M.; Krocher, O. Effect of SiO_2 on co-impregnated $V_2O_5/WO_3/TiO_2$ catalysts for the selective catalytic reduction of NO with NH_3. *Catal. Today* **2019**, *320*, 123–132. [CrossRef]
2. Forzatti, P. Present status and perspectives in de-NO_x SCR catalysis. *Appl. Catal. A Gen.* **2001**, *222*, 221–236. [CrossRef]
3. Wang, S.; Xie, Y.; Yan, W.; Wu, X.; Wang, C.; Zhao, F. Leaching of vanadium from waste V_2O_5-WO_3/TiO_2 catalyst catalyzed by functional microorganisms. *Sci. Total Environ.* **2018**, *639*, 497–503. [CrossRef] [PubMed]
4. Li, M.; Liu, B.; Wang, X.; Yu, X.; Zheng, S.; Du, H. A promising approach to recover a spent SCR catalyst: Deactivation by arsenic and alkaline metals and catalyst regeneration. *Chem. Eng. J.* **2018**, *342*, 1–8. [CrossRef]
5. Choi, I.; Kim, H.; Moon, G.; Jyothi, R.; Lee, J. Spent V_2O_5-WO_3/TiO_2 catalyst processing for valuable metals by soda roasting-water leaching. *Hydrometallurgy* **2018**, *175*, 292–299. [CrossRef]
6. Xiao, C.; Zeng, L.; Wei, J.; Xiao, L.; Zhang, G. Thermodynamic analysis for the separation of tungsten and aluminum in alkaline medium using solvent extraction. *Hydrometallurgy* **2017**, *174*, 91–96. [CrossRef]
7. Luo, L.; Liu, K.; Shibayama, A.; Yen, W.; Fujita, T.; Shindo, O. Recovery of tungsten and vanadium from tungsten alloy scrap. *Hydrometallurgy* **2004**, *72*, 1–8. [CrossRef]
8. Wu, W.; Tsai, T.; Shen, Y. Tungsten Recovery from Spent SCR Catalyst Using Alkaline Leaching and Ion Exchange. *Minerals* **2016**, *6*, 107. [CrossRef]
9. Tang, D.; Song, H.; Liu, D.; Wu, W.; Zheng, C.; Gao, X. Study on leaching kinetics of extracting vanadium and tungsten by sodium hydroxide from spent SCR catalyst. *Chin. J. Environ. Eng.* **2017**, *11*, 1093–1100.
10. Su, Q.; Miao, J.; Li, H.; Chen, Y.; Chen, J.; Wang, J. Optimizing vanadium and tungsten leaching with lowered silicon from spent SCR catalyst by pre-mixing treatment. *Hydrometallurgy* **2018**, *181*, 230–239. [CrossRef]
11. Wang, J.; Miao, J.; Yu, W.; Chen, Y.; Chen, J. Study on the local difference of monolithic honeycomb V_2O_5-WO_3/TiO_2 denitration catalyst. *Mater. Chem. Phys.* **2017**, *198*, 193–199. [CrossRef]
12. Lietti, L.; Ramis, G.; Berti, F.; Toledo, G.; Robba, D.; Busca, G. Chemical, structural and mechanistic aspects on NO_x SCR over commercial and model oxide catalysts. *Catal. Today* **1998**, *42*, 101–116. [CrossRef]
13. Kwon, D.; Park, K.; Hong, S. The influence on SCR activity of the atomic structure of V_2O_5/TiO_2 catalysts prepared by a mechanochemical method. *Appl. Catal. A Gen.* **2013**, *451*, 227–235. [CrossRef]
14. Zong, L.; Dong, F.; Zhang, G.; Han, W.; Tang, Z.; Zhang, J. Highly Efficient Mesoporous V_2O_5/WO_3-TiO_2 Catalyst for Selective Catalytic Reduction of NO_x: Effect of the Valence of V on the Catalytic Performance. *Catal. Surv. Asia* **2017**, *21*, 103–113. [CrossRef]
15. Lietti, L.; Forzatti, P.; Bregani, F. Steady-State and Transient Reactivity Study of TiO_2-Supported V_2O_5−WO_3 De-NO_x Catalysts: Relevance of the Vanadium−Tungsten Interaction on the Catalytic Activity. *Ind. Eng. Chem. Res.* **1996**, *35*, 3884–3892. [CrossRef]
16. Li, Q.; Liu, Z.; Liu, Q. Kinetics of Vanadium Leaching from a Spent Industrial V_2O_5/TiO_2 Catalyst by Sulfuric Acid. *Ind. Eng. Chem. Res.* **2014**, *53*, 2956–2962. [CrossRef]
17. Zhang, Q.; Wu, Y.; Li, L.; Zuo, T. Sustainable Approach for Spent V_2O_5–WO_3/TiO_2 Catalysts Management: Selective Recovery of Heavy Metal Vanadium and Production of Value-Added WO_3–TiO_2 Photocatalysts. *ACS Sustain. Chem. Eng.* **2018**, *6*, 12502–12510. [CrossRef]
18. Wu, W.; Wang, C.; Bao, W.; Li, H. Selective reduction leaching of vanadium and iron by oxalic acid from spent V_2O_5-WO_3/TiO_2 catalyst. *Hydrometallurgy* **2018**, *179*, 52–59. [CrossRef]
19. Dong, G.; Bai, Y.; Zhang, Y.; Zhao, Y. Effect of the $V^{4+(3+)}/V^{5+}$ ratio on the denitration activity for V_2O_5-WO_3/TiO_2 catalysts. *New J. Chem.* **2015**, *39*, 3588–3596. [CrossRef]
20. Chen, H.; Xia, Y.; Fang, R.; Huang, H.; Gan, Y.; Liang, C. The effects of tungsten and hydrothermal aging in promoting NH_3-SCR activity on V_2O_5/WO_3-TiO_2 catalysts. *Appl. Surf. Sci.* **2018**, *459*, 639–646. [CrossRef]
21. Zhang, S.; Zhong, Q. Surface characterization studies on the interaction of V_2O_5-WO_3/TiO_2 catalyst for low temperature SCR of NO with NH_3. *J. Solid State Chem.* **2015**, *221*, 49–56. [CrossRef]
22. Dong, G.; Zhang, Y.; Zhao, Y.; Bai, Y. Effect of the pH value of precursor solution on the catalytic performance of V_2O_5-WO_3/TiO_2 in the low temperature NH_3-SCR of NO_x. *J. Fuel Chem. Technol.* **2014**, *42*, 1455–1463. [CrossRef]

23. Kompio, P.; Brueckner, A.; Hipler, F.; Manoylova, O.; Auer, G.; Mestl, G. V_2O_5-WO_3/TiO_2 catalysts under thermal stress: Responses of structure and catalytic behavior in the selective catalytic reduction of NO by NH_3. *Appl. Catal. B Environ.* **2017**, *217*, 365–377. [CrossRef]
24. Ren, F.; Li, H.; Wang, Y.; Yang, J. Enhanced photocatalytic oxidation of propylene over V-doped TiO_2 photocatalyst: Reaction mechanism between V^{5+} and single-electron-trapped oxygen vacancy. *Appl. Catal. B Environ.* **2015**, *176*, 160–172. [CrossRef]
25. Mendialdua, J.; Casanova, R.; Barbaux, Y. XPS Studies of V_2O_5, V_6O_{13}, VO_2 and V_2O_3. *J. Electron Spectrosc. Phenom.* **1995**, *71*, 249–261. [CrossRef]
26. Szymczycha, A. Kinetics of Mo, Ni, V and Al leaching from a spent hydrodesulphurization catalyst in a solution containing oxalic acid and hydrogen peroxide. *J. Hazard. Mater.* **2011**, *186*, 2157–2161. [CrossRef]
27. Yaws, C.L. Chapter 2—Physical Propert—Inorganic Compounds. In *The Yaws Handbook of Physical Properties for Hydrocarbons and Chemicals*, 2nd ed.; Gulf Professional Publishing: Boston, MA, USA, 2015; pp. 684–810.
28. Zhou, X.; Wei, C.; Xia, W.; Li, M.; Li, C.; Deng, Z. Dissolution kinetics and thermodynamic analysis of vanadium trioxide during pressure oxidation. *Rare Metals* **2012**, *31*, 296–302. [CrossRef]
29. Xue, Y.; Zhang, Y.; Zhang, Y.; Zheng, S.; Zhang, Y.; Jin, W. Electrochemical detoxification and recovery of spent SCR catalyst by in-situ generated reactive oxygen species in alkaline media. *Chem. Eng. J.* **2017**, *325*, 544–553. [CrossRef]
30. Qiu, S.; Wei, C.; Li, M.; Zhou, X.; Li, C.; Deng, Z. Dissolution kinetics of vanadium trioxide at high pressure in sodium hydroxide-oxygen systems. *Hydrometallurgy* **2011**, *105*, 350–354. [CrossRef]
31. Zhou, X.; Wei, C.; Li, M.; Qiu, S.; Li, X. Thermodynamics of vanadium–sulfur–water systems at 298K. *Hydrometallurgy* **2011**, *106*, 104–112. [CrossRef]
32. Madia, G.; Elsener, M.; Koebel, M.; Raimondi, F.; Wokaun, A. Thermal stability of vanadia-tungsta-titania catalysts in the SCR process. *Appl. Catal. B Environ.* **2002**, *39*, 181–190. [CrossRef]